Journal of Alloys and Compounds 683 (2016) 186–190

Contents lists available at ScienceDirect

Journal of Alloys and Compounds

journal homepage: http://www.elsevier.com/locate/jalcom

Acetone gas sensor based on α-Ag_2WO_4 nanorods obtained via a microwave-assisted hydrothermal route

Luís F. da Silva [a, *], Ariadne C. Catto [b], Waldir Avansi Jr. [c], Laécio S. Cavalcante [d], Valmor R. Mastelaro [b], Juan Andrés [e], Khalifa Aguir [f], Elson Longo [a]

[a] LIEC, Instituto de Química, Universidade Estadual Paulista, P.O. Box 355, 14800-900, Araraquara, SP, Brazil
[b] Instituto de Física de São Carlos, Universidade de São Paulo, Avenida Trabalhador São-carlense, 400, 13566-590, São Carlos, SP, Brazil
[c] Departamento de Física, Universidade Federal de São Carlos, Rodovia Washington Luiz, São Carlos, SP, Brazil
[d] DQ-GERATEC-Universidade Estadual do Piauí, 64002-150, Teresina, PI, Brazil
[e] Departamento de Química-Física y Analitica, Universitat Jaume I, Campus de Riu Sec, Castelló, E-12080, Spain
[f] Aix Marseille Université, CNRS IM2NP (UMR 7334), FS St Jérôme S152, Marseille, 13397, France

ARTICLE INFO

Article history:
Received 7 February 2016
Received in revised form
27 April 2016
Accepted 8 May 2016
Available online 10 May 2016

Keywords:
Microwave-assisted hydrothermal
α-Ag_2WO_4
Nanorods
Gas sensor
Acetone

ABSTRACT

This manuscript addresses the synthesis of one-dimensional (1D) α-Ag_2WO_4 nanorod-like structures via a microwave-assisted hydrothermal method to be used as an acetone gas sensor. The nanorods showed excellent gas-sensing performance, evidenced by their sensor response and repeatability, as well as a good range of detection (0.5–20.0 ppm). The manuscript also proposes an easy and efficient way of obtaining 1-D α-Ag_2WO_4 nanorods that exhibit remarkable acetone sensing properties.

1. Introduction

Over the past decades, inorganic semiconducting nanostructures have drawn interest from the research community driven by their physical and chemical properties, which enable their use in light-emission/detection devices, gas sensors, biomedical devices, and battery electrodes [1–6]. Among different nanostructures, one-dimensional (1D) semiconducting materials, such as nanorods, nanowires, and nanotubes must be highlighted because of their distinctive geometries and fascinating properties [1,7–11]. Their synthesis has been carried out by various chemical and/or physical methods [7,12–14], among which the microwave-assisted hydrothermal (MAH) method has proven efficient, fast and versatile for the obtaining of organic and inorganic materials [2,7,15–17].

Silver tungstate (Ag_2WO_4) compounds have attracted widespread scientific and technological interest, especially regarding their multifunctional applications [2,16,18–25]. In a previous study, we reported the gas-sensing performance of such 1D α-Ag_2WO_4 nanorod-like structures obtained by MAH route, which detected lower concentrations of ozone, i.e., 80 ppb [2]. Regarding gas sensing applications, the main advantage of 1D nanostructures is their high surface-to-volume ratio, which favors the adsorption of gases on their surface [26], enhances their sensing performance and enables the detection of lower gas concentrations [26–28].

Over the past years, breath analysis has been utilized as a useful tool for the noninvasive diagnosis and monitoring of a broad range of diseases [29–31]. Acetone is a specific breath marker for diabetes, therefore, gas sensors have been used for the detection of acetone levels in the human breath [29,30,32]. Its concentration ranges between 0.3 and 0.9 ppm for healthy humans, whereas it is found in higher concentrations, i.e., >1.8 ppm in diabetic patients [29,30,33]. Efforts have been devoted towards the discovery of novel acetone-sensing compounds, or enhancement of the gas sensing performance of traditional acetone gas sensor devices [1,29–32,34–41]. As shown in Table 1, different semiconducting metal oxides have been investigated as acetone gas sensor, as displayed in Table 1.

* Corresponding author.
E-mail address: lfsilva83@gmail.com (L.F. da Silva).

http://dx.doi.org/10.1016/j.jallcom.2016.05.078
0925-8388/

Table 1
Brief summary of results reported for acetone gas sensors based on semiconducting metal oxides.

Compound	Acetone level (ppm)	Operating temp. (°C)	References
ZnO	1–500	350	[1]
ZnO	1000–3000	325	[40]
ZnO–CuO	0.2–50	310	[41]
WO_3:Si	0.1–0.6	350	[33]
ZnO:Mn	50–300	300	[34]
$ZnFe_2O_4$	0.8–50	200	[39]
α-Fe_2O_3	1–5	350	[31]

This manuscript addresses the gas sensing properties of 1D α-Ag_2WO_4 nanorod-like structures obtained by MAH route. The morphological characteristics of as-prepared nanorods were analyzed by field emission scanning electron microscopy (FE-SEM). The α-Ag_2WO_4 nanorods were tested for the detection of acetone, ethanol, and ammonia. The gas sensing experiments performed at 350 °C revealed their higher sensitivity to acetone in comparison to other gases, fast response-recovery time and excellent repeatability.

2. Experimental

2.1. Preparation and characterization of α-Ag_2WO_4 nanorods

The synthesis of silver tungstate (α-Ag_2WO_4) nanostructures was accomplished using the were prepared by the microwave-assisted hydrothermal (MAH) treatment method, using $AgNO_3$ (99.8%), $Na_2WO_4.2H_2O$ (99.5%), and PVP40 ($(C_6H_9NO)_n$; 99%) as reagents. The precursor α-Ag_2WO_4 solution was heat-treated in microwave hydrothermal equipment for 1 h at 160 °C. Further details of the synthesis procedure may be found in Ref. [2]. The sample was structurally characterized by X-ray diffraction (XRD) using CuKa radiation (Rigaku diffractometer, model D/Max-2500PC) in a 2θ range from 10° to 60° with a step of 0.02°at a scanning speed of $2°min^{-1}$. The morphological features of the α-Ag_2WO_4 nanostructures were analyzed under a field emission scanning electron microscope (FE-SEM; FEI INSPECT F50) operating at 20 kV and by transmission electron microscopy (TEM) on a JEM 2010 URP operating at 200 kV.

2.2. Sensor preparation and gas-sensing measurements

The α-Ag_2WO_4 powder was dispersed in isopropyl alcohol for 30 min by an ultrasonic cleaner and the suspension was dripped onto an SiO_2/Si substrate containing 100 nm thick Pt electrodes separated by a 50 mm distance. The sample was then annealed in an electric furnace for 2 h under air atmosphere at 500 °C.

The sensor sample was inserted into a gas sensing chamber for the control of both temperature and gas flow. The working temperature, which ranged from 250 °C to 350 °C, was maintained by an external heating source driven by a regulated power supply. A 1 V dc voltage was applied to the device while the electrical resistance was being monitored by a Keithley (model 6514) electrometer.

The acetone concentration was controlled through the mixing of acetone vapor with synthetic air at different ratios for the gas-sensing measurements. The desired gas concentration was obtained through the injection of the amount of liquid acetone required (Quemis, 99.5%) into a sealed glass container by a syringe. Dry air was used as both a reference (baseline) and a carrier gas and 8.3 cm^3 s^{-1} constant total flow was maintained by mass flow controllers. The relative humidity inside the chamber was monitored by a commercial sensor (INSTRUTHERM, HT-700) and held at approximately 85%.

The sensor response, S, was defined as $S = R_{air}/R_{gas}$, where R_{air} and R_{gas} are the electrical resistances of the sensor device exposed to dry air and acetone gas. The response time of the sensor was defined as the time required for a change in the sample's electrical resistance to reach 90% of the initial value when exposed to acetone. Similarly, the recovery time was defined as the time required for the electrical resistance of the sensor to reach 90% of the initial value after the acetone has been turned off.

3. Results and discussion

3.1. Structural, microstructural and gas-sensing properties

Fig. 1 shows the X-ray diffraction (XRD) patterns of α-Ag_2WO_4 nanostructures obtained via MAH route. All diffraction peaks were indexed to an orthorhombic structure with a *Pn2n* space group, according to ICSD file 4165, as expected [22].

FE-SEM image confirms the morphology of the α-Ag_2WO_4 sample, which consists of uniform and one-dimensional (1D) rod-like structures, as illustrated in the inset of Fig. 1(b) and (c). The average width and length of the nanorods were approximately 100 nm and 1.5 μm, as reported in our previously work [2]. The presence of Ag nanoparticles on the α-Ag_2WO_4 nanorods' surfaces (Fig. 1c) is due to their exposition to electron irradiation under an SEM microscope [20–22]. Nevertheless, the as-prepared nanorods used in the gas sensor tests were not exposed to electron irradiation.

First, the sensor response of α-Ag_2WO_4 nanorods was investigated for 10 ppm of acetone at a fixed operating temperature of 300 °C and different exposition times (15 s, 60 s, 90 s, and 5 min), as shown in Fig. 2a. Upon exposure to acetone vapor, the electrical resistance of the nanorods quickly decreased, which is a typical response of *n*-type semiconductors exposed to reducing gases [29]. Additionally, the nanorods showed a good sensor response for short periods of time and tended toward saturation only for longer exposure times (>90 s), as shown in Fig. 2a. This behavior can be explained by the limited number of adsorption sites on the nanorods' surface.

The α-Ag_2WO_4 sample was then exposed to 10 ppm of acetone at a fixed time of 60 s, so that the best operating temperature could be found. Such exposition time was chosen because the sensor response did not vary significantly for longer times. The results in Fig. 2b show an increase of the sensor response in function of the operating temperature – the maximum response was obtained at 350 °C, which is the limit of our gas sensing system. Righettoni and co-workers investigated the acetone gas-sensing properties of Si-doped WO_3 nanoparticles prepared via flame spray pyrolysis method and observed the highest sensor response at 350 °C [30]. The gas sensing measurements performed at various operating temperatures are displayed in Fig. S1.

Fig. 3 shows the dynamic sensor resistance of the α-Ag_2WO_4 nanorods under exposure to various concentrations of acetone (0.5–20 ppm) at 350 °C. The reversible cycles of the response curves indicate a stable and reproducible response, as seen in Fig. 3a. The sensor response gradually increases with the increase in the concentration of acetone, which suggests the nanorods have not reached saturation, even for higher concentrations of up to 20 ppm, Fig. 3b. Additionally, the response time and recovery time ranged between 30–32 s and 46–130 s, respectively, towards various acetone concentrations.

In order to investigate the selectivity of sensor, α-Ag_2WO_4 nanorods were exposed at 350 °C to acetone, ethanol, and ammonia at the concentration level of 10 ppm. The electrical measurements

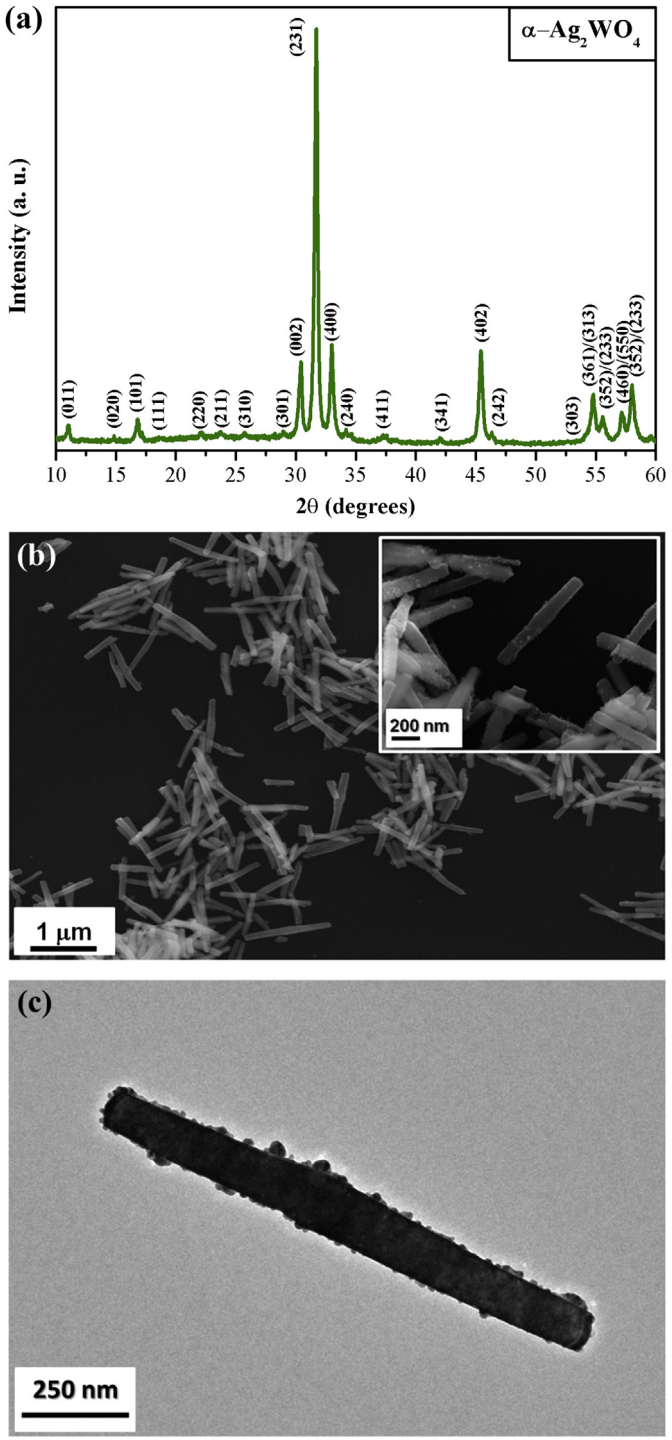

Fig. 1. The α-Ag_2WO_4 sample prepared via MAH treatment method. (a) XRD pattern, (b) FESEM image, and (c) TEM image.

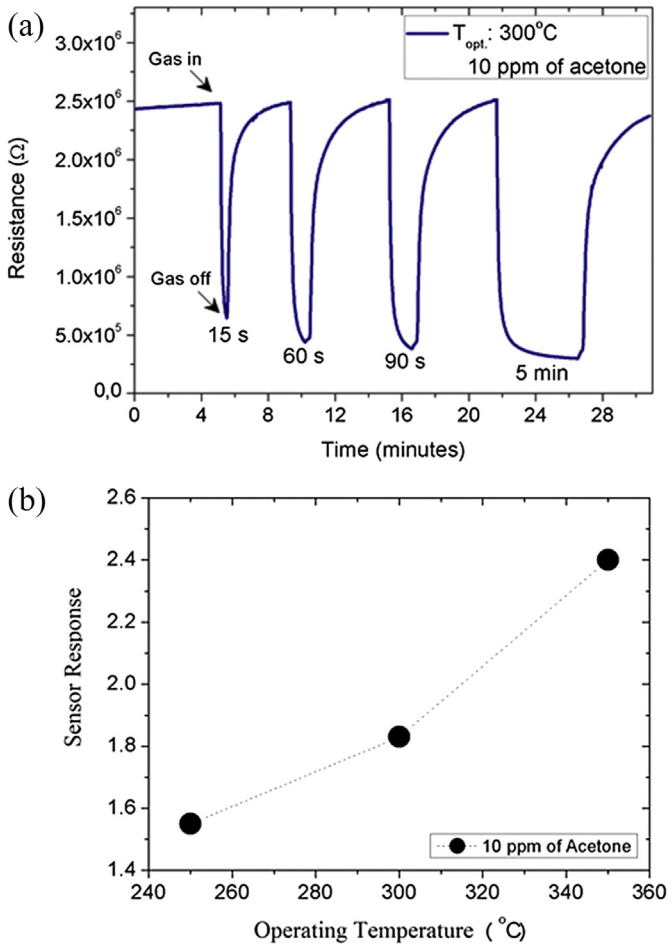

Fig. 2. (a) Electrical resistance of α-Ag_2WO_4 nanorods upon exposure to 10 ppm acetone for differing times at an operating temperature of 300 °C. (b) Sensor response *vs.* operating temperatures.

are displayed in the Fig. S2, respectively. According to Fig. 4, the nanorods were sensitive for all gases, exhibiting the highest sensitivity to acetone when compared to other gases under the same concentration. The sensor response obtained was, 2.77 ± 0.04 (acetone), 1.69 ± 0.02 (ethanol), and 1.57 ± 0.05 (ammonia).

Initially, when the sample is exposed to an air atmosphere, the oxygen molecules are adsorbed on the different α-Ag_2WO_4 surfaces, resulting in the formation of oxygen ionic species, such as O_2^-, O^-, O^{2-} [42]. In our experiments, the operating temperatures, $T_{opt.}$, was varied from 250 °C to 350 °C, and thus the ionic species O^- are dominant [43]. These O^- species contribute to form a depletion layer in the nanorods surfaces, leading to high resistance [27]. In the sequence, upon exposure to acetone, CH_3COCH_3 molecules will react with the chemisorbed oxygen ions at the nanorods surfaces. As consequence, the charge carrier is increased and, the depletion layer is diminished, leading to a decrease in electrical resistance [43,31]. The acetone gas sensing mechanism of the α-Ag_2WO_4 nanorods can be explained by:

$$O_{2(gas)} + 2e^- \rightarrow 2O^-_{(ads)} \quad (1)$$

$$CH_3COCH_{3(gas)} + 8O^- \rightarrow 3CO_{2(g)} + 3H_2O_{(liq)} + 8e^- \quad (2)$$

3.2. Final remarks applying for future investigations

As the α-Ag_2WO_4 compound is a potential gas sensor device, the way intrinsic factors, as type of crystalline structure (alpha, beta, and gamma) also affect the gas sensing performance in silver tungstate should be investigated. Future approaches on Ag_2WO_4 characteristics should also include analyses of the plasmonic effect on gas sensing properties, i.e., presence of Ag metallic nanoparticles grown on the nanorods surfaces due to their exposition to electron irradiation under an SEM microscope.

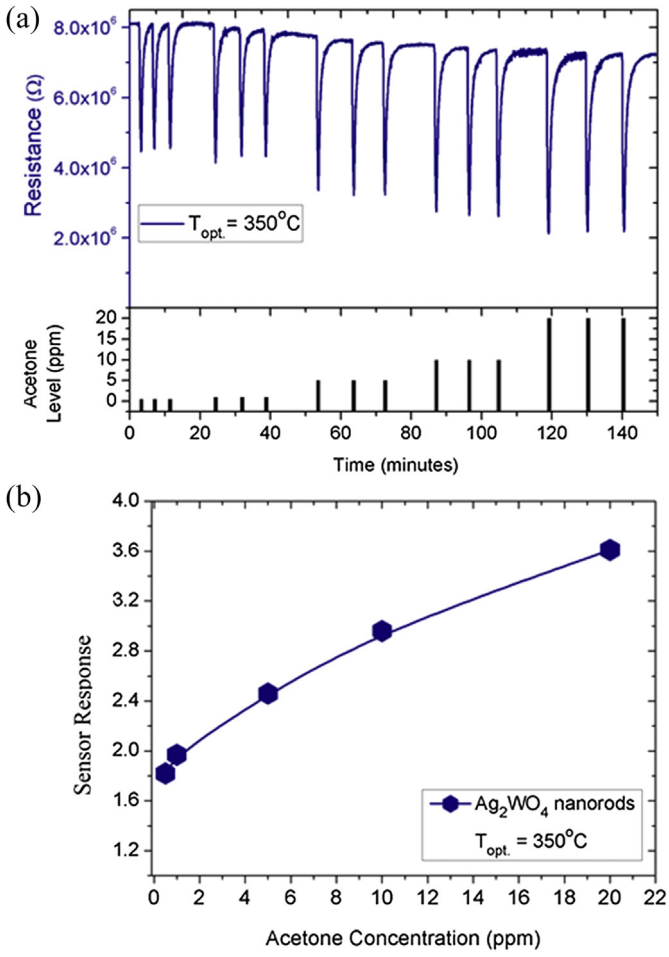

Fig. 3. Acetone gas-sensing response for the α-Ag_2WO_4 nanorods. (a) Electrical resistance and (b) sensor response vs. acetone concentration at 350 °C.

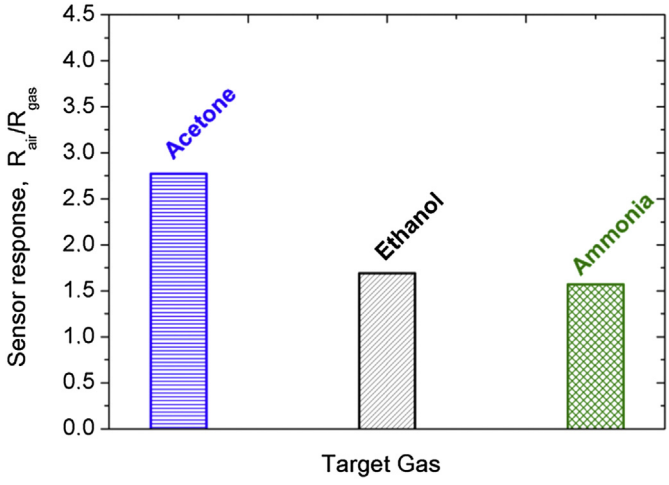

Fig. 4. Sensor response of the α-Ag_2WO_4 nanorods towards acetone, ethanol, and ammonia.

4. Conclusion

This paper reported on a fast and effective approach for the preparation of acetone gas sensors based on 1D α-Ag_2WO_4 nanostructures via a microwave-assisted hydrothermal method. XRD and FE-SEM analyses revealed the presence of a crystalline phase of α-Ag_2WO_4 that exhibits a rod-like morphology. Gas sensing measurements showed the good acetone sensing performance of such nanorods at an operating temperature of 350 °C. The nanorods detected different acetone levels that ranged from 0.5 ppm to 20 ppm and showed a fast response (of ca. 30 s), excellent repeatability, and great potential for practical applications.

Acknowledgments

We are grateful for the financial support from Brazilian research funding agencies CNPq and FAPESP (under grants No. 2013/09573-3, 2013/07296-2, 2012/15170-6, 479644/2012-8, 442076/2014-2, and 304531/2013-8). This research was partially performed at the Brazilian Nanotechnology National Laboratory (LNNano), Microfabrication laboratory (Project 17168), Campinas, SP, Brazil. J. Andrés acknowledges Generalitat Valenciana (Prometeo/2009/053 project), Ministerio de Ciencia e Innovacion (CTO2009-14541-C02 project) Programa de Cooperacion Científica con Iberoamerica (Brazil), and Ministerio de Educacion (PHB2009-0065-PC project).

Appendix A. Supplementary data

Supplementary data related to this article can be found at http://dx.doi.org/10.1016/j.jallcom.2016.05.078.

References

[1] M.R. Alenezi, S.J. Henley, N.G. Emerson, S.R.P. Silva, From 1D and 2D ZnO nanostructures to 3D hierarchical structures with enhanced gas sensing properties, Nanoscale 6 (2014) 235–247, http://dx.doi.org/10.1039/c3nr04519f.
[2] L.F. da Silva, A.C. Catto, W. Avansi, L.S. Cavalcante, J. Andres, K. Aguir, et al., A novel ozone gas sensor based on one-dimensional (1D) α-Ag_2WO_4 nanostructures, Nanoscale 6 (2014) 4058–4062, http://dx.doi.org/10.1039/C3NR05837A.
[3] C.N.R. Rao, F.L. Deepak, G. Gundiah, A. Govindaraj, Inorganic nanowires, Prog. Solid State Chem. 31 (2003) 5–147, http://dx.doi.org/10.1016/j.progsolidstchem.2003.08.001.
[4] G.R. Patzke, F. Krumeich, R. Nesper, Oxidic nanotubes and nanorods–anisotropic modules for a future nanotechnology, Angew. Chem. Int. Ed. 41 (2002) 2446–2461, http://dx.doi.org/10.1002/1521-3773.
[5] S. Maeng, S.-W. Kim, D.-H. Lee, S.-E. Moon, K.-C. Kim, A. Maiti, SnO_2 nanoslab as NO_2 sensor: identification of the NO_2 sensing mechanism on a SnO_2 surface, ACS Appl. Mater. Interfaces 6 (2014) 357–363, http://dx.doi.org/10.1021/am404397f.
[6] A.P. Alivisatos, Semiconductor clusters, nanocrystals, and quantum dots, Science 271 (1996) 933–937, http://dx.doi.org/10.1126/science.271.5251.933.
[7] I. Bilecka, M. Niederberger, Microwave chemistry for inorganic nanomaterials synthesis, Nanoscale 2 (2010) 1358–1374, http://dx.doi.org/10.1039/B9NR00377K.
[8] S. Salehi, E. Nikan, A.A. Khodadadi, Y. Mortazavi, Highly sensitive carbon nanotubes–SnO_2 nanocomposite sensor for acetone detection in diabetes mellitus breath, Sens. Actuators B Chem. 205 (2014) 261–267, http://dx.doi.org/10.1016/j.snb.2014.08.082.
[9] Y. Cui, Q. Wei, H. Park, C.M. Lieber, Nanowire nanosensors for highly sensitive and selective detection of biological and chemical species, Science 293 (2001) 1289–1292, http://dx.doi.org/10.1126/science.1062711.
[10] X. Peng, L. Manna, W. Yang, J. Wickham, E. Scher, A. Kadavanich, et al., Shape control of CdSe nanocrystals, Nature 404 (2000) 59–61, http://dx.doi.org/10.1038/35003535.
[11] Z.A. Peng, X. Peng, Nearly Monodisperse and Shape-Controlled CdSe Nanocrystals via alternative Routes: nucleation and growth, J. Am. Chem. Soc. 124 (2002) 3343–3353, http://dx.doi.org/10.1021/ja0173167.
[12] A. Tricoli, M. Righettoni, A. Teleki, Semiconductor gas sensors: dry synthesis and application, Angew. Chem. Int. Ed. 49 (2010) 7632–7659, http://dx.doi.org/10.1002/anie.200903801.
[13] C. Burda, X. Chen, R. Narayanan, M.A. El-Sayed, Chemistry and properties of nanocrystals of different shapes, Chem. Rev. 105 (2005) 1025–1102, http://dx.doi.org/10.1021/cr030063a.
[14] M. Niederberger, Nonaqueous sol–gel routes to metal oxide nanoparticles, Acc. Chem. Res. 40 (2007) 793–800, http://dx.doi.org/10.1021/ar600035e.
[15] I. Bilecka, L. Luo, I. Djerdj, M.D. Rossell, M. Jagodič, Z. Jagličić, et al., Microwave-assisted nonaqueous Sol–Gel chemistry for highly concentrated ZnO-based magnetic semiconductor nanocrystals, J. Phys. Chem. C 115 (2011) 1484–1495, http://dx.doi.org/10.1021/jp108050w.

[16] L.F. da Silva, W. Avansi, M.L. Moreira, J. Andres, E. Longo, V.R. Mastelaro, Novel $SrTi_{1-x}Fe_xO_3$ nanocubes synthesized by microwave-assisted hydrothermal method, CrystEngComm 14 (2012) 4068–4073, http://dx.doi.org/10.1039/C2CE25229E.
[17] G.A. Tompsett, W.C. Conner, K.S. Yngvesson, Microwave synthesis of nanoporous materials, ChemPhysChem 7 (2006) 296–319, http://dx.doi.org/10.1002/cphc.200500449.
[18] R.A. Roca, J.C. Sczancoski, I.C. Nogueira, M.T. Fabbro, H.C. Alves, L. Gracia, et al., Facet-dependent photocatalytic and antibacterial properties in α-Ag_2WO_4 crystals: combining experimental data and theoretical insights, Catal. Sci. Technol. (2015), http://dx.doi.org/10.1039/C5CY00331H.
[19] Wda S. Pereira, J. Andres, L. Gracia, M.A. San-Miguel, E.Z. da Silva, E. Longo, et al., Elucidating the real-time Ag nanoparticle growth on [small alpha]-Ag_2WO_4 during electron beam irradiation: experimental evidence and theoretical insights, Phys. Chem. Chem. Phys. 17 (2015) 5352–5359, http://dx.doi.org/10.1039/C4CP05849F.
[20] J. Andres, L. Gracia, P. Gonzalez-Navarrete, V.M. Longo, W. Avansi Jr., D.P. Volanti, et al., Structural and electronic analysis of the atomic scale nucleation of Ag on α-Ag_2WO_4 induced by electron irradiation, Sci. Rep. 4 (2014) 5391, http://dx.doi.org/10.1038/srep05391.
[21] E. Longo, L.S. Cavalcante, D.P. Volanti, A.F. Gouveia, V.M. Longo, J.A. Varela, et al., Direct in situ observation of the electron-driven synthesis of Ag filaments on α-Ag_2WO_4 crystals, Sci. Rep. 3 (2013), http://dx.doi.org/10.1038/srep01676.
[22] E. Longo, D.P. Volanti, V.M. Longo, L. Gracia, I.C. Nogueira, M.A.P. Almeida, et al., Toward an understanding of the growth of Ag filaments on α-Ag_2WO_4 and their photoluminescent properties: a combined experimental and theoretical study, J. Phys. Chem. C 118 (2014) 1229–1239, http://dx.doi.org/10.1021/jp408167v.
[23] Z. Lin, J. Li, Z. Zheng, J. Yan, P. Liu, C. Wang, et al., Electronic reconstruction of α-Ag_2WO_4 nanorods for the visible-light photocatalysis, ACS Nano (2015), http://dx.doi.org/10.1021/acsnano.5b02077.
[24] K. Vignesh, M. Kang, Facile synthesis, characterization and recyclable photocatalytic activity of Ag_2WO_4@g-C_3N_4, Mater. Sci. Eng. B 199 (2015) 30–36, http://dx.doi.org/10.1016/j.mseb.2015.04.009.
[25] D.P. Dutta, A. Singh, A. Ballal, A.K. Tyagi, High adsorption capacity for cationic dye removal and antibacterial properties of sonochemically synthesized Ag_2WO_4 nanorods, Eur. J. Inorg. Chem. 2014 (2014) 5724–5732, http://dx.doi.org/10.1002/ejic.201402612.
[26] X. Zhou, S. Lee, Z. Xu, J. Yoon, Recent progress on the development of chemosensors for gases, Chem. Rev. (2015), http://dx.doi.org/10.1021/cr500567r.
[27] A.C. Catto, L.F. da Silva, C. Ribeiro, S. Bernardini, K. Aguir, E. Longo, et al., An easy method of preparing ozone gas sensors based on ZnO nanorods, RSC Adv. 5 (2015) 19528–19533, http://dx.doi.org/10.1039/C5RA00581G.
[28] X. Li, Y. Chang, Y. Long, Influence of Sn doping on ZnO sensing properties for ethanol and acetone, Mater. Sci. Eng. C 32 (2012) 817–821, http://dx.doi.org/10.1016/j.msec.2012.01.032.
[29] M. Righettoni, A. Tricoli, S. Gass, A. Schmid, A. Amann, S.E. Pratsinis, Breath acetone monitoring by portable Si:WO_3 gas sensors, Anal. Chim. Acta 738 (2012) 69–75, http://dx.doi.org/10.1016/j.aca.2012.06.002.
[30] M. Righettoni, A. Tricoli, S.E. Pratsinis, Si:WO_3 sensors for highly selective detection of acetone for easy diagnosis of diabetes by breath analysis, Anal. Chem. 82 (2010) 3581–3587, http://dx.doi.org/10.1021/ac902695n.
[31] D.H. Kim, Y.-S. Shim, J.-M. Jeon, H.Y. Jeong, S.S. Park, Y.-W. Kim, et al., Vertically ordered hematite nanotube array as an ultrasensitive and rapid response acetone sensor, ACS Appl. Mater. Interfaces 6 (2014) 14779–14784, http://dx.doi.org/10.1021/am504156w.
[32] S.-J. Choi, I. Lee, B.-H. Jang, D.-Y. Youn, W.-H. Ryu, C.O. Park, et al., Selective diagnosis of diabetes using Pt-Functionalized WO_3 hemitube networks As a sensing layer of acetone in exhaled breath, Anal. Chem. 85 (2013) 1792–1796, http://dx.doi.org/10.1021/ac303148a.
[33] M. Righettoni, A. Tricoli, Toward portable breath acetone analysis for diabetes detection, J. Breath. Res. 5 (2011) 37109. http://stacks.iop.org/1752-7163/5/i=3/a=037109.
[34] M.H. Darvishnejad, A. Anaraki Firooz, J. Beheshtian, A.A. Khodadadi, Highly sensitive and selective ethanol and acetone gas sensors by adding some dopants (Mn, Fe, Co, Ni) onto hexagonal ZnO plates, RSC Adv. 6 (2016) 7838–7845, http://dx.doi.org/10.1039/C5RA24169C.
[35] X. Chi, C. Liu, L. Liu, Y. Li, Z. Wang, X. Bo, et al., Tungsten trioxide nanotubes with high sensitive and selective properties to acetone, Sens. Actuators B Chem. 194 (2014) 33–37, http://dx.doi.org/10.1016/j.snb.2013.12.078.
[36] Y. Zhang, W. He, H. Zhao, P. Li, Template-free to fabricate highly sensitive and selective acetone gas sensor based on WO_3 microspheres, Vacuum 95 (2013) 30–34, http://dx.doi.org/10.1016/j.vacuum.2013.02.005.
[37] L. Wang, A. Teleki, S.E. Pratsinis, P.I. Gouma, Ferroelectric WO_3 nanoparticles for acetone selective detection, Chem. Mater 20 (2008) 4794–4796, http://dx.doi.org/10.1021/cm800761e.
[38] L. Xu, M.-L. Yin, S. (Frank) Liu, Superior sensor performance from Ag@WO_3 core–shell nanostructure, J. Alloy. Compd. 623 (2015) 127–131, http://dx.doi.org/10.1016/j.jallcom.2014.10.103.
[39] X. Zhou, J. Liu, C. Wang, P. Sun, X. Hu, X. Li, et al., Highly sensitive acetone gas sensor based on porous $ZnFe_2O_4$ nanospheres, Sens. Actuators B Chem. 206 (2015) 577–583, http://dx.doi.org/10.1016/j.snb.2014.09.080.
[40] P.P. Sahay, Zinc oxide thin film gas sensor for detection of acetone, J. Mater. Sci. 40 (2005) 4383–4385, http://dx.doi.org/10.1007/s10853-005-0738-0.
[41] Y. Xie, R. Xing, Q. Li, L. Xu, H. Song, Three-dimensional ordered ZnO–CuO inverse opals toward low concentration acetone detection for exhaled breath sensing, Sens. Actuators B Chem. 211 (2015) 255–262, http://dx.doi.org/10.1016/j.snb.2015.01.086.
[42] H.-J. Kim, J.-H. Lee, Highly sensitive and selective gas sensors using p-type oxide semiconductors: Overview, Sens. Actuators B Chem. 192 (2014) 607–627, http://dx.doi.org/10.1016/j.snb.2013.11.005.
[43] D. Chen, L. Ge, L. Yin, H. Shi, D. Yang, J. Yang, et al., Solvent-regulated solvothermal synthesis and morphology-dependent gas-sensing performance of low-dimensional tungsten oxide nanocrystals, Sens. Actuators B Chem. 205 (2014) 391–400, http://dx.doi.org/10.1016/j.snb.2014.09.007.